Oriented Immobilization of a Membrane-Bound Hydrogenase onto an Electrode for Direct Electron Transfer

ARTICLE *in* LANGMUIR · MAY 2011

Impact Factor: 4.46 · DOI: 10.1021/la200141t · Source: PubMed

7 AUTHORS, INCLUDING:

David Olea
AlphaSip Aragon
37 PUBLICATIONS **832** CITATIONS
SEE PROFILE

Marta Marques
Instituto de Medicina Molecular
22 PUBLICATIONS **300** CITATIONS
SEE PROFILE

Inês Cardoso Pereira
New University of Lisbon
99 PUBLICATIONS **2,155** CITATIONS
SEE PROFILE

Antonio De Lacey
Spanish National Research Council
90 PUBLICATIONS **3,682** CITATIONS
SEE PROFILE

Langmuir

ARTICLE

pubs.acs.org/Langmuir

Oriented Immobilization of a Membrane-Bound Hydrogenase onto an Electrode for Direct Electron Transfer

Cristina Gutiérrez-Sánchez,[†,∥] David Olea,[†,∥] Marta Marques,[§] Victor M. Fernández,[†] Inês A. C. Pereira,[§] Marisela Vélez,[†,‡] and Antonio L. De Lacey*[,†]

[†]Instituto de Catálisis y Petroleoquímica, CSIC, C/Marie Curie 2, 28049 Madrid, Spain

[‡]Instituto Madrileño de Estudios Avanzados en Nanociencia (IMDEA-Nanociencia), Facultad de Ciencias, C-IX-3[a] Cantoblanco 28049, Madrid, Spain

[§]Instituto de Tecnologia Química e Biológica, Universidade Nova de Lisboa, Apartado 127, 2781-901 Oeiras, Portugal

Supporting Information

ABSTRACT: The interaction of redox enzymes with electrodes is of great interest for studying the catalytic mechanisms of redox enzymes and for bioelectronic applications. Efficient electron transport between the biocatalysts and the electrodes has achieved more success with soluble enzymes than with membrane enzymes because of the higher structural complexity and instability of the latter proteins. In this work, we report a strategy for immobilizing a membrane-bound enzyme onto gold electrodes with a controlled orientation in its fully active conformation. The immobilized redox enzyme is the Ni−Fe−Se hydrogenase from *Desulfovibrio vulgaris* Hildenborough, which catalyzes H_2-oxidation reversibly and is associated with the cytoplasmic membrane by a lipidic tail. Gold surfaces modified with this enzyme and phospholipids have been studied by atomic force microscopy (AFM) and electrochemical methods. The combined study indicates that by a two-step immobilization procedure the hydrogenase can be inserted via its lipidic tail onto a phospholipidic bilayer formed over the gold surface, allowing only mediated electron transfer between the enzyme and electrode. However, a one-step immobilization procedure favors the formation of a hydrogenase monolayer over the gold surface with its lipidic tail inserted into a phospholipid bilayer formed on top of the hydrogenase molecules. This latter method has allowed for the first time efficient electron transfer between a membrane-bound enzyme in its native conformation and an electrode.

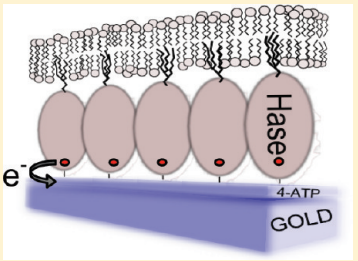

INTRODUCTION

Over the last few decades, much research has focused on developing suitable interfaces that are able to link biochemical processes catalyzed by redox enzymes to electrochemical ones, with the aim of improving the charge transport between the biocatalysts and the electrodes. The optimization of these interfaces allows the study of the catalytic mechanisms of redox enzymes[1,2] and bioelectronic applications.[3,4] This field has achieved more success with soluble enzymes than with membrane enzymes because of the higher structural complexity and instability of the latter proteins. Two general approaches have been used to interface membrane enzymes with electrodes: physisorption on electrodes, generally graphite ones, and immobilization on membrane-modified electrodes.[5] The first approach has been successful in measuring direct electron transfer between the electrode and the hydrophilic subunits of some membrane enzymes.[6,7] However, by this method the way that the membrane enzyme is bound to the electrode is uncertain, and there is no control over whether the enzyme maintains its integral conformation. Besides, the measured catalytic currents or the protein stability on the electrode is often low.[6−8] However, the immobilization of redox membrane enzymes on gold electrodes modified with model membranes has allowed the electrochemical study of these enzymes in a lipidic environment, which maintains their structural and functional integrity.[9−11] However, by this latter strategy direct electron transfer between the enzymes and electrodes was not detected or was very sluggish, thus requiring the use of redox mediators. The reason for this is that these methods led to an orientation of the enzyme that is not optimal for direct electron transfer (DET), placing the redox center too far away from the electrode surface.[5]

Hydrogenases catalyze the oxidation of H_2 and its production from protons with almost no overpotential.[12] Therefore, their immobilization on electrodes holds potential interest for the development of biological fuel cells, electrolytic cells, and hydrogen biosensors.[13] Many strategies have been reported for immobilizing hydrogenases on electrodes, such as physical adsorption,[14−18] covalent bonding,[19,20] entrapment in redox polymers,[21,22] and layer-by-layer deposition.[23,24] Charge exchange between the electrode and the hydrogenase has been achieved in some strategies by DET,[14−18,20] whereas it has been achieved in others by mediated electron transfer (MET).[19,21−24]

Received: January 12, 2011
Revised: March 31, 2011
Published: April 14, 2011

In previous work, we have developed a robust, controlled immobilization method for the soluble hydrogenase from *Desulfovibrio gigas* onto different types of electrodes on the basis of electrostatic interactions directing the correct orientation of the enzyme for DET.[20,25,26] This method exploits the negative surface region found around the distal 4Fe4S cluster of the hydrogenase. This cluster connects the enzyme surface to the buried Ni−Fe active site through an electron-transport chain formed by two other FeS clusters.[27] We now report a specific immobilization method for a membrane-bound hydrogenase: the Ni−Fe−Se hydrogenase isolated from *D. vulgaris* Hildenborough. This hydrogenase is associated with the cytoplasmic membrane of the organism and displays interesting catalytic properties, such as a high H_2-production activity in the presence of phospholipids or detergents and fast reductive reactivation after exposure to oxygen.[28,29] The enzyme is post-transcriptionally modified to include a lipidic group bound to the N terminus of the large subunit, which allows for its association with the membrane.[30] The activity of this enzyme is very dependent on the presence of detergent or phospholipids in the medium, suggesting that the lipidic group plays an important structural role in optimal catalysis.[28] Cleavage of the first few residues of the large subunit (including the lipidic group) produces a soluble, but less active, form of the hydrogenase. This cleavage can occur spontaneously, particularly when detergent is removed from the enzyme.

The goal of the present work was to covalently bind membrane *Desulfovibrio vulgaris* Hildenborough Ni−Fe−Se hydrogenase to an electrode while maintaining its most active form with the intact lipidic group and at the same time controlling its correct orientation for DET. Previously, we have shown that electrocatalytic current densities measured with the membrane form of this hydrogenase, covalently bound to SAM-modified gold electrodes, were 1 order of magnitude lower than those obtained with the soluble *D. gigas* Ni−Fe hydrogenase.[26] This occurred in spite of the higher activity of the former enzyme in solution over the latter one, especially for H_2 production.[28] As mentioned above, this high catalytic activity of the membrane-bound hydrogenase depends on the preservation of its lipidic tail under the measurement conditions. Therefore, these preliminary results suggested that the immobilization procedure was not optimal for a membrane-bound enzyme, leading to a less active form of the hydrogenase on the electrode.

To retain the maximum activity of the immobilized membrane-bound hydrogenase on solid supports, we have implemented a strategy to anchor the protein and induce the formation of a protective lipid bilayer on the electrode. A combined atomic force microscopy (AFM) and electrochemical study of this process under different conditions was used to verify the efficiency of the procedure. The use of a flat, conductive support, such as Au(111), allowed the simultaneous evaluation of the morphology of the enzyme-coated electrodes and their electrocatalytic properties.

METHODS

Enzyme Purification. *D. vulgaris* Hildenborough Ni−Fe−Se hydrogenase was purified and biochemically characterized as described by Valente et al.[28] The membrane form (intact enzyme containing the lipidic tail) and the soluble form (lacking the first 12 residues of the large subunit and the lipidic tail) of the enzyme were separated as described by Marques et al.[31] Enzyme solutions contained 50 mM tris(hydroxymethyl)aminomethane buffer at pH 7.6, 100 mM NaCl, and 0.1 wt % *N*-dodecyl β-D-maltoside.

Reagents. All reagents purchased were analytical grade. Hydrogen peroxide 30%, H_2SO_4 98%, absolute ethanol, $Na_2HPO_4 \cdot 12H_2O$, and $NaH_2PO_4 \cdot 2H_2O$ were purchased from Panreac. 4-Aminothiophenol (4-ATP) and *N*-hydroxysuccinimide (NHS) were from Fluka. Methyl viologen (MV), *N*-(3-dimethylaminopropyl)-*N*′-ethylcarbodiimide hydrochloride (EDC), *N*-dodecyl β-D-maltoside (DDM), and MES hydrate 99.5% were supplied by Sigma-Aldrich. *Escherichia coli* polar lipids were purchased from Avanti. CALBIOSORB Adsorbent was purchased from Calbiochem. Poly(ethylene glycol) *tert*-octylphenyl ether (Triton X-100) was supplied by Fluka. Octadecyl (C_{18}) indocarbocyanine (DiI) was purchased from Molecular Probes. All aqueous solutions were prepared in deionized water (Milli-Q grade).

Gold Surface Preparation. Au-coated substrates (1 × 1 cm^2) were purchased from Metallhandel Schroer GMBH. They consist of 200 nm gold over 1−4 nm of chromium prepared on borosilicate glass. The substrates were cleaned with piranha solution (3:1 H_2SO_4 98%/H_2O_2 30%) and rinsed extensively with Milli Q water. (***Caution!*** *Piranha solution is especially dangerous and corrosive and may explode if contained in a closed vessel. It should be handled with special care.*) The substrates were then annealed to an orange glow for a few seconds in a propane flame; this operation was repeated five times. This treatment is known to produce Au(111) terraces of a few micrometers' radius with atomically flat surfaces separated by deep boundaries, suitable for atomic force microscopy (AFM) characterization. Gold wires with a radius of 0.25 mm were purchased from Goodfellow Cambridge Limited and treated as the Au-coated substrates.

Covalent Immobilization of the Membrane Hydrogenase to 4-ATP-Modified Gold. A 4-ATP self-assembled monolayer (SAM) was formed by immersing Au(111) substrates in a 1 mM 4-ATP solution in ethanol for 18 h at room temperature. The substrates were then rinsed with ethanol and dried with N_2. The substrates' surfaces (0.2 cm^2) were then incubated for 20 min with 15 μL of a 27 μM hydrogenase solution in 10 mM MES buffer at pH 6 and 0.1 wt % DDM to allow the enzyme to bind to the 4-ATP-modified gold surface through electrostatic interactions. Then, 17 μL of 21 mM ECD and 14 μL of 14 mM NHS in the same buffer were added to the solution. After 30 min of the coupling reaction, the substrates were finally rinsed with a 0.1 M phosphate at pH 7.0, 0.25 M KCl buffer solution.

Preparation of Liposomes. A 10 mg/mL chloroform solution of *E. coli* polar fraction phospholipids (Avanti) was evaporated using N_2. Milli-Q water was then added in order to form a 4 mg/mL suspension of phospholipids that was submitted to ultrasound for 15 min. The suspension was then extruded with an Avanti extruder equipped with a porous membrane (pores diameter of 300 nm). This procedure leads to the formation of a quasi-monodisperse suspension of unilamelar vesicles.[32] The dispersion was then diluted to 0.6 mg/mL with 10 mM MES buffer at pH 5.

Insertion of Hydrogenase in a Phospholipidic Bilayer Formed over Gold. A 4-ATP SAM was formed on the Au(111) surface as described above. The gold substrates were then incubated with the 0.6 mg/mL liposome dispersion in 10 mM MES buffer at pH 5 for 15 min and rinsed with 0.1 M PBS buffer. This procedure led to the formation of a phospholipidic bilayer on the gold surface. Afterwards, 0.2 cm^2 of the substrate surface was incubated for 60 min with 18 μL of 27 μM *D. vulgaris* Hildenborough Ni−Fe−Se hydrogenase solution in 10 mM MES buffer at pH 6 and 48 mg of CALBIOSORB Adsorbent. The gold samples were finally washed with a 0.1 M PBS buffer solution.

Hydrogenase and Phospholipids Coimmobilization on Gold Surfaces. Twelve microliters of 27 μM hydrogenase in 10 mM MES buffer at pH 6 and 0.1wt % of DDM were mixed with 20 μL of a 0.6 mg/mL liposome dispersion in 10 mM MES buffer at pH 5, and immediately 48 mg of CALBIOSORB Adsorbent were added. A few

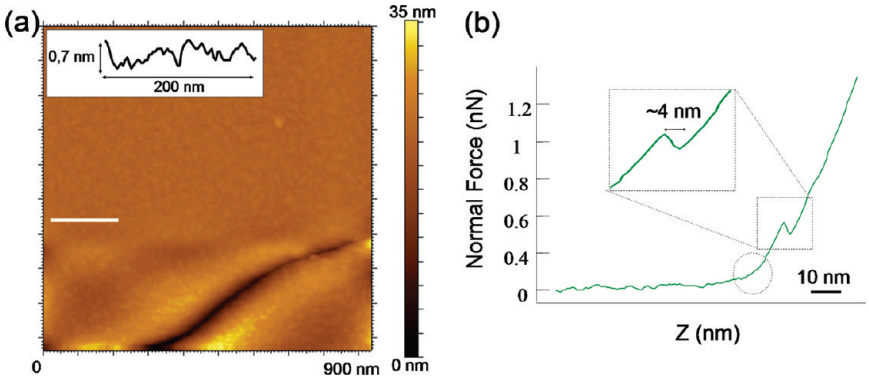

Figure 1. (a) Tapping-mode AFM topography of a phospholipidic bilayer formed on a 4-ATP-functionalized gold (111) surface. The inset represents the *z*-axis profile across the line drawn. (b) Force−distance (*z* axis) curve acquired over a flat gold area. The circle indicates the part of the curve corresponding to the contact between the AFM tip and the surface. The square indicates the portion of the curve associated with the bilayer rupture.

seconds later, 0.2 cm^2 of a 4-ATP-modified Au(111) substrate surface was incubated for 20 min with the mixed solution. The substrates were then incubated with a solution of 11.6 mM ECD in 10 mM MES buffer at pH 6 for 30 min. To remove noncovalently immobilized hydrogenase molecules, the modified gold surface was intensively washed with 0.1 M PBS buffer solution. The same method was used to modify the gold wires.

Electrochemical Measurements. Electrochemical experiments were run in a three-electrode glass cell with a saturated calomel reference electrode (SCE) separated from the main compartment in a side arm connected by a Luggin capillary. The cell temperature was controlled by a water jacket. A platinum wire was used as a counter electrode. This set up keeps the reference electrode at room temperature so the potentials can be converted to SHE by using the correction factor $E_{SHE} = E_{SCE} + 0.241$ V. All of the measurements were performed inside a Mbraun glovebox with an oxygen content of <1 ppm, and the gases used (H_2, N_2, and CO from Air Liquide) were flushed through an oxygen filter (Varian) before entering the electrochemical cell. The potentiostat/galvanostat used was an Autolab PGSTAT30 or a μ-Autolab III electrochemical analyzer controlled by GPES software (Eco Chemie). Gold wires or the gold-covered plates used for AFM characterization were used as working electrodes. The current densities are calculated by taking into account the geometrical area of the working electrodes.

Atomic Force Microscopy (AFM) Study. An Agilent Technologies (Santa Clara, CA) 5500 microscope was used for AFM imaging. Measurements were always made under liquid conditions in PBS buffer at room temperature using Olympus rectangular silicon nitride cantilevers (RC800PSA, 200 × 20 μm^2) with a spring constant of 0.05 N/m, an estimated tip radius of 20 nm, and a resonance frequency in the liquid cell of approximately 27 kHz. Scanning rates were kept close to 1 Hz. All images contain 512 pixels × 512 pixels and were first-order flatterned using Picoimage software from Agilent.

Florescence Microscopy and Fluorescence Recovery after Photobleaching (FRAP) Measurements. FRAP experiments were performed using a model eclipse E600FN Nikon microscope provided with a D-FL EPI-fluorescence attachment. For all fluorescence measurements of the lipid bilayers, we added 2 wt % of the DiI fluorophore to the polar fraction of *E. coli* phospholipids. The lipid bilayers were formed on polycrystalline gold (previously cleaned with piranha solution and treated with 4-ATP). A circular area with a radius of 48 μm was photobleached by using full lamp power for 1 min. We measured the intensity of the photobleached area and a reference area in all images in order to normalize the photobleached area measurements that would otherwise be minimized by the intrinsic photobleaching due to imaging. The normalized photobleached area intensity at time *t*, *I*, was calculated using the equation $I = I_{pt} + (I_{ref0} - I_{ref})$, where I_{pt} was the photobleached area intensity at time *t*, I_{ref0} was the reference area intensity immediately after photobleaching, and I_{ref} was the reference area intensity at time *t*. We used an exponential function to fit the fluorescence recovery. After calculating the half-life recovery, $t_{1/2}$, the equation $D = 0.224r^2/t_{1/2}$ (with *r* being the radius of the photobleached area) was used to calculate the phospholipids diffusion coefficient, *D*.[33]

RESULTS AND DISCUSSION

Covalent Immobilization of the Membrane Hydrogenase to 4-ATP-Modified Gold. Covalent immobilization of the membrane *D. vulgaris* Ni−Fe−Se hydrogenase by the method already developed for soluble hydrogenases[26] and in presence of a noncharged detergent necessary for preserving its lipidic tail led to the formation of a hydrogenasse monolayer on the gold surface as observed by AFM (Figure S1a). However, the DET electrocatalytic current densities of H_2 oxidation in this case were low (Figure S1b). These results suggest that this method leads to the immobilization of the membrane hydrogenase in a conformation that does not allow optimal electrocatalytic activity. Although the immobilization of the hydrogenase monolayer was done in presence of detergent, the electrocatalytic measurements were made in a solution without detergent to avoid foam formation during the saturation of the solution with H_2, which causes poor electrochemical conditions. Therefore, this method probably results in some cleavage of the lipidic tail of the immobilized hydrogenase during the measurement, leading to a less-active enzyme.

Formation of a Phospholipidic Bilayer on the Gold Surface. To try to immobilize the hydrogenase in a catalytically optimal state, the formation of a phospholipidic bilayer on the gold surface was attempted. The self-assembly of lipid bilayers on untreated gold surfaces does not take place spontaneously.[34] However, Cha et al. succeeded in forming lipid bilayers on gold decorated with alkanethiols functionalized with amino groups and negatively charged liposomes.[35] Accordingly, we studied the formation of a bilayer on a 4-ATP-modified surface (at a pH lower than the pK_a of its amino groups[36] so that positive charges would be present on the gold surface) using negatively charged *E. coli* phospholipids. The AFM topographic images show an almost featureless surface after incubating a 4-ATP-modified gold surface with phospholipids (Figure 1a). The topographic profile of the surface within a terrace is provided (inset of Figure 1a), showing height variations smaller than 1 nm. The root-mean-square rugosity remains comparable to that of the untreated

dx.doi.org/10.1021/la200141t |*Langmuir* 2011, 27, 6449–6457

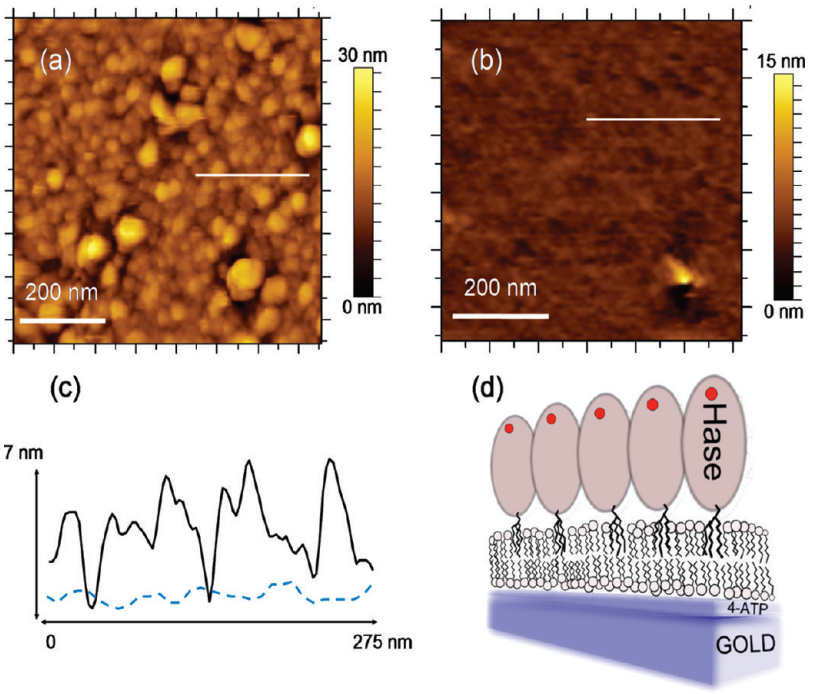

Figure 2. Tapping-mode AFM topographic images of a phospholipidic membrane on 4-ATP-modified Au(111) after incubation with the *D. vulgaris* Ni−Fe−Se hydrogenase (a) membrane form or (b) soluble form for 45 min in the presence of CALBIOSORB Adsorbent. (c) *z*-axis profiles are drawn in a (black line) and in b (cyan line). (d) Schematic representation of the insertion of hydrogenase molecules in the phospholipidic bilayer. The red circles represent the distal 4Fe4S clusters.

4-ATP gold substrate (not shown). The thickness of the material deposited on top of the 4-ATP layer was studied by recording force−distance ($F-Z$) curves inside different gold terraces. In this indentation experiment, the AFM tip is set a certain distance from the surface and is then approached at a constant speed as the deflection of the cantilever is recorded. Figure 1b shows a representative $F-Z$ indentation curve taken on a gold terrace. The flat first part of the curve corresponds to the moment when the AFM tip and the surface are not interacting. As the tip approaches the surface, a repulsive interaction between the tip and the immobilized material is first established (part of the curve marked with a circle), followed by a region in which the response of the cantilever to the increasing pressure of the moving substrate is linear. The point of rupture, detected by the discontinuity in the slope, reflects a change in the mechanical properties of the material lying under the tip. The force at which this rupture takes place in the range of 1 ± 0.5 nN, and the 4 nm penetration depth of the tip on the softer material (part of the curve marked with a square) is compatible with the behavior described for a tip penetrating and breaking a 4-nm-thick lipid bilayer deposited on a hard surface.[37−39]

Insertion of the Membrane Hydrogenase in the Phospholipidic Bilayer Supported on Gold. The phospholipidic bilayer-modified gold substrates were incubated with a solution of detergent-solubilized membrane hydrogenase and the CALBIOSORB Adsorbent, which consists of patented millispheres that are able to adsorb a large variety of surfactants without affecting phospholipids.[40] The use of this product was crucial because it removes the DDM surfactant, which otherwise could dissolve the lipid bilayer. After incubation, the membrane surface was roughened, as shown in Figure 2a. The globular disposition of the hydrogenase molecules over the surface is observed, with a mean height close to 5 nm and a mean lateral size of approximately 100 nm (Figure 2c). The height of the globules fits well with the longer diameter of the hydrogenase molecule determined by X-ray diffraction[41] and with other AFM and STM studies.[18,42] Although the vertical resolution of AFM is about 0.3 nm, the lateral resolution is given by the convolution of the tip (with a radius of 20 nm). Thus, it is not possible to ascertain if the observed globules are composed of one or several molecules of hydrogenase. We find that the hydrogenase molecules were immobilized by the insertion of their lipidic tails into the phospholipid bilayer as shown in the scheme of Figure 2d. Further experiments were subsequently done to support this hypothesis.

The catalytic function of the hydrogenase immobilized in the bilayer-modified gold was evaluated electrochemically. The gold plate was used as the working electrode in an electrochemical cell. Figure 3a shows cyclic voltammograms (CV) recorded with this electrode under different conditions. In the absence of a redox mediator in solution, hardly any difference is observed between the CV measured under H_2 and N_2 (red and black lines, respectively). This is a clear indication that the electrocatalytic oxidation of H_2 by DET between the enzyme and the electrode does not take place. However, in the presence of 0.16 mM MV, a standard redox mediator used for the electrochemistry of hydrogenases,[19,20,23,24] a clear catalytic effect due to an oxidative reaction that starts at negative potential values is observed when comparing the CV under H_2 and N_2 (blue and green lines, respectively). The CV in the presence of H_2 and MV has a peaked shape instead of the sigmoidal shape expected for an electrocatalytic process, probably because of mass-transfer limitations of H_2 toward the electrode (the solution is quiescent). After the addition of 44 μM CO, the electrocatalytic process is almost totally surpressed (cyan line). This result confirms that the electrocatalytic

dx.doi.org/10.1021/la200141t |*Langmuir* 2011, 27, 6449–6457

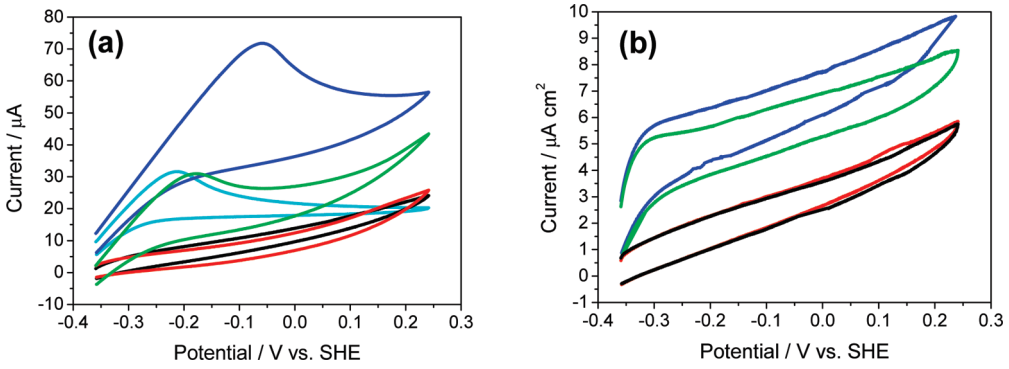

Figure 3. Cyclic voltammograms (CV) of gold plates modified with 4-ATP/phospholipidic membrane after incubation with the *D. vulgaris* Ni−Fe−Se hydrogenase (a) membrane form or (b) soluble form. The black and red lines correspond to the CV measured in the absence of a redox mediator under 1 atm of N_2 and H_2, respectively. The green and blue lines correspond to the CV measured in the presence of 0.16 mM methyl viologen under 1 atm of N_2 and H_2, respectively. The cyan line corresponds to the CV in presence of 0.16 mM methyl viologen and 44 μM CO under 1 atm of H_2. The measurements were made in 0.1 M phosphate buffer at pH 6 at a 20 mV s^{-1} scan rate and 40 °C.

process (blue line) is due to the H_2-oxidation activity of the immobilized hydrogenase because CO is a strong inhibitor of its catalytic activity.[29] Thus, the immobilized hydrogenase molecules were catalytically active in H_2 oxidation, although they were not able to transfer electrons directly to the electrode. Instead, they reduced the MV molecules in solution, and these were subsequently oxidized at the electrode during the CV scan toward positive potentials, causing the electrocatalytic wave observed. The phospholipid bilayer is thus permeable to the diffusion of MV. This suggests that there are defects in the membrane allowing the access of MV to the electrode. In fact, the presence of defects in the phospholipid bilayer is detected in the AFM study shown and discussed in the next subsection. In the Supporting Information, we show an electrochemical study of the permeability of this bilayer toward different redox mediators (Figure S2).

The electrochemical results support the orientation of the immobilized hydrogenase shown in Figure 2d in which the lipidic tail is inserted within the phospholipidic bilayer and its distal 4Fe4S cluster (located in the protein region opposite the lipidic tail)[41] is facing the solution. In hydrogenases, the distal 4Fe4S cluster is the redox center that exchanges electrons with the redox partner during the catalytic cycle.[12,13,20] In the orientation of hydrogenase molecules shown in Figure 2d, these redox centers are too far from the electrode surface for effective DET but are well placed for electron exchange with the redox mediator in solution.

A control experiment was performed by incubating the bilayer-modified gold surface with the soluble form of the *D. vulgaris* Ni−Fe−Se hydrogenase that is missing the lipidic tail.[28] The AFM study showed that in this case the samples had an almost featureless surface, only differentiable from the lipid bilayer by the presence of a few aggregates (Figure 2b). The rugosity is similar to that of the lipid bilayer over gold (Figure 2c). In addition, electrochemical measurements showed that in this case there was no electrocatalytic activity of H_2 oxidation by DET and hardly any by MET (Figure 3b). Thus, both AFM and electrochemical measurements indicate that the lipidic tail of the hydrogenase is responsible for its immobilization on the bilayer-modified gold surface. All of these observations lead to the conclusion that we have achieved the immobilization of catalytically active hydrogenase molecules onto the phospholipid bilayer-modified surface by the insertion of its lipidic tail with the orientation shown in Figure 2d. This conformation probably mimics the in vivo situation in which the membrane-bound hydrogenase is anchored to the cytoplasmic cell membrane via its lipidic tail and the distal 4Fe4S cluster is facing the periplasm for electron exchange with its soluble physiological partner (type I cytochrome c_3).[28]

Hydrogenase and Phospholipid Co-immobilization on Gold Surfaces. The previous experiments showed that the addition of the hydrogenase to a preformed bilayer-coated electrode stabilizes the immobilized enzyme in an active conformation but results in an enzyme orientation that does not allow DET. Thus, we developed an alternative strategy for the coimmobilization of the enzyme and phospholipids in one step. It was expected that incubating the positively charged 4-ATP-modified gold substrate in a hydrogenase solution in the presence of phospholipids could favor the electrostatic orientation of the hydrogenase molecules on the surface according to the protein surface dipole moment[26] and at the same time allow the stabilization of their lipidic tails by interaction with the phospholipids added to the solution. In this way, the negatively charged distal 4Fe4S cluster region of the hydrogenase would be facing the gold surface whereas the lipidic tail would be facing the solution. Again, the presence of CALBIOSORB Adsorbent millispheres were necessary for the substitution of the DDM detergent by the phospholipids, allowing for stabilization of the hydrogenase in its most active form. This strategy is inspired by that reported by Levy et al. for the formation of 2D crystals of membrane proteins on modified surfaces. Slow detergent removal from a solution containing a membrane protein with lipids and detergent allowed protein orientation on a surface, modified with an anchoring group, and the simultaneous formation of the surrounding lipid bilayer.[43]

An AFM topographic image of the gold surface after immobilization of the hydrogenase molecules in the presence of *E. coli* polar phospholipids is given in Figure 4a. A surprisingly flat surface is observed, with no evidence at all of the presence of hydrogenase molecules. Furthermore, no features except holes were found in many areas of six different samples. The rugosity of the samples, not taking into account the holes, was very low with a value of $Rq = 0.7 \pm 0.4$ nm (Figure 4c, black line). The height of the deepest holes found in the membrane is on the order of 12 nm, which is the expected height of the full construction represented in Figure 4d. Holes with smaller heights are also detected, such as the 6 nm one illustrated in Figure 4c (black

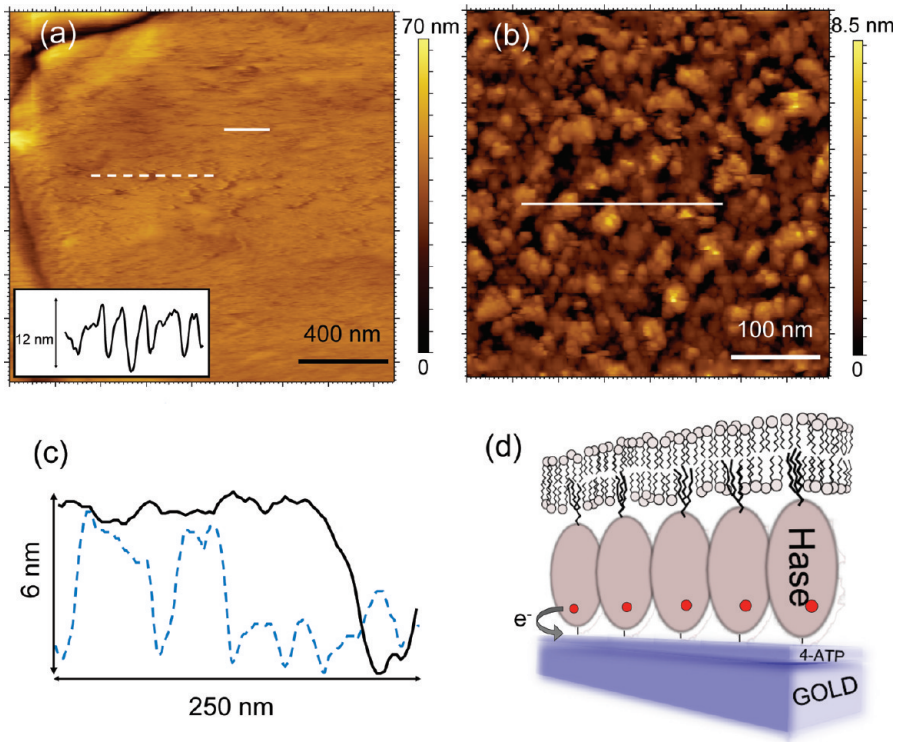

Figure 4. (a) Tapping-mode AFM topography of a 4-ATP-modified gold plate to which membrane hydrogenase has been covalently immobilized in the presence of phospholipids and CALBIOSORB Adsorbent. The inset represents the *z*-axis profile across the dashed white line. (b) AFM topography of the same system after 2 min of incubation with 1 μM Triton X100. (c) *z*-axis profiles across the solid lines in a (black line) and b (cyan line). (d) Scheme depicting the covalent and oriented immobilization of hydrogenase molecules with the subsequent formation of a membrane on top of the proteins. The direct electron transfer between the active center of the enzyme and the electrode is represented.

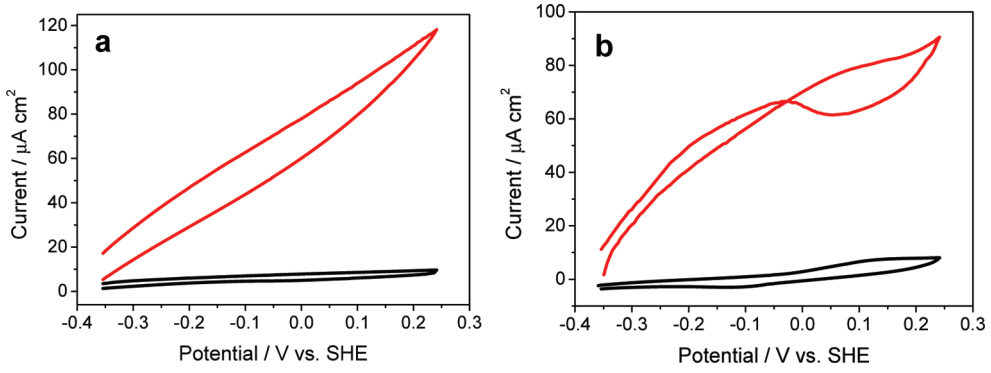

Figure 5. CV of (a) a 4-ATP-modified gold plate and (b) a wire to which membrane hydrogenase has been covalently immobilized in the presence of phospholipids and the CALBIOSORB Adsorbent. The measurements were made in 0.1 M phosphate buffer at pH 6 under 1 atm of N_2 (black lines) or 1 atm of H_2 (red lines) at a 20 mV s^{-1} scan rate and 40 °C.

line), which could represent incomplete regions in which either the protein or the full bilayer is missing. We do not detect deeper holes that would indicate the formation of stacked bilayers. The small height of the defects supports our hypothesis of the formation of a single lipid bilayer on top of the oriented and immobilized proteins. To prove this hypothesis, the samples were treated with Triton X-100, a tensioactive known for solubilizing lipid bilayers.[44,45] This procedure led to the recovery of a globular appearance of the modified gold samples, as shown by AFM imaging (Figure 4b). Small platelets with a height of 5 to 6 nm corresponding to fragments of the lipid bilayer that resisted the Triton X-100 effect are present on top of the globular background (Figure 4c, cyan dashed line). Therefore, the AFM study is in agreement with an oriented hydrogenase monolayer bound directly to the 4-ATP-modified gold surface, over which a phospholipidic bilayer was self-assembled using the lipidic hydrogenase tails as a scaffold, as shown in Figure 4d. In the Supporting Information, we show AFM images on the same *z* scale of the modified gold surface before and after removal of the phospholipid bilayer with Triton X-100 (Figure S3).

Again, electrochemical measurements were used to evaluate the catalytic function of the immobilized hydrogenase and to check its orientation relative to the conductive surface. Figure 5a shows the CV of the gold plates with coimmobilized membrane

dx.doi.org/10.1021/la200141t |*Langmuir* 2011, 27, 6449–6457

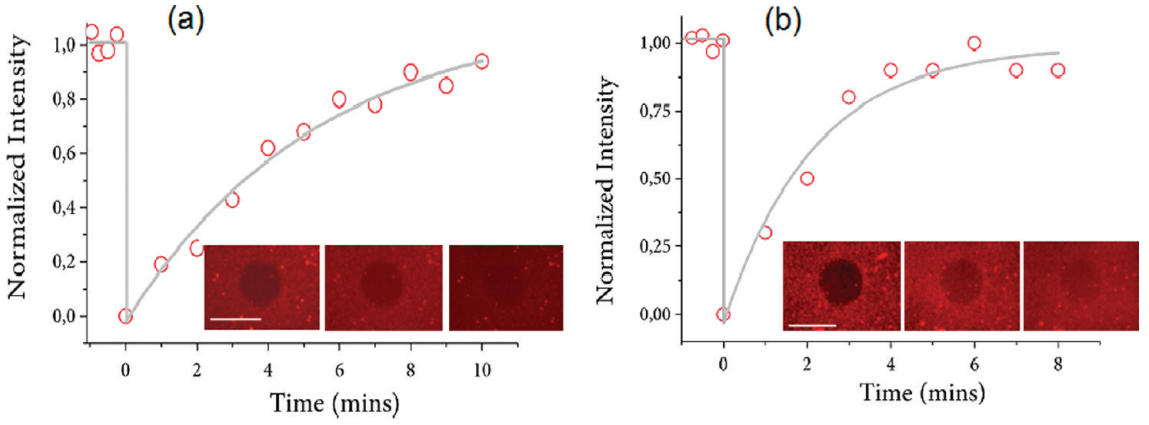

Figure 6. FRAP data from a lipid bilayer (a) supported on a 4-ATP-modified gold substrate or (b) formed on top of hydrogenase molecules covalently immobilized on 4-ATP-modified gold. The insets represent the corresponding fluorescence micrographs of the photobleached area at $t = 0$, 4, and 8 min. The scale bar is 8 μm.

hydrogenase and phospholipids under N_2 (black line) or under H_2 (red line) in the absence of redox mediators. The results clearly show that the hydrogenase immobilized by this strategy can catalyze the oxidation of H_2 by DET. Thus, the electrochemical measurements are in agreement with the architecture shown schematically in Figure 4d in which the hydrogenase molecules are preferentially oriented with the distal 4Fe4S clusters facing the gold electrode surface, although the exact distance between this redox center and the electrode may vary from one enzyme molecule to another because there are several carboxylic residues surrounding the distal 4Fe4S cluster that can form covalent bonds.

Moreover, the catalytic current densities measured by DET with this strategy are significantly enhanced compared to those obtained with the membrane hydrogenase covalently bound to the 4-ATP-modified gold in the absence of phospholipids (Figure S1b). This suggests that the phospholipid bilayer assembled over the hydrogenase monolayer stabilizes the enzyme in its most active form by interaction with the lipidic tail.

CV measurements were also made using a polycrystalline gold wire as a support for the coimmobilization of hydrogenase and phospholipids. The gold wire has a lower ohmic resistance than the gold nanolayer on the AFM plates, it has a more suitable geometry for the diffusion of the H_2 substrate toward the electrode, and it has a higher surface rugosity that may increase the DET rate with the immobilized hydrogenase. Figure 5b shows the CV measured with this type of electrode. The CV performed under N_2 shows low capacitive currents, in agreement with an electrode surface completely covered with a supramolecular assembly. A faint faradaic process with an anodic peak at +100 mV and a cathodic peak at approximately −150 mV is also detected. It could correspond to one of the 4Fe4S clusters of the immobilized hydrogenase, although it appears at higher potentials than would be expected.[46] No H_2 production catalyzed by the hydrogenase is observed under a N_2 atmosphere because the CV was not scanned to redox potentials lower than −350 mV in order to avoid the reductive desorption of the 4-ATP monolayer from the gold surface.[26] In contrast, under H_2, a high electrocatalytic oxidation process that starts at −350 mV is observed because of the immobilized hydrogenase activity. A pseudoplateau current density of approximately 80 μA/cm^2 is reached at +50 mV, considering the geometrical area of the gold wire (0.15 cm^2). This value is approximately 20 times higher than that measured in a previous work with the same membrane hydrogenase covalently bound to a gold electrode in the absence of phospholipids and of the same order of magnitude as that measured with a soluble hydrogenase.[26] Besides, a gradual decrease in the catalytic current can be observed in the reverse scan of the CV from 250 to 0 mV; subsequently, there is sigmoidal increase in the catalytic current as the potential is swept to lower potentials. This particular shape of the CV was reproducible for several modified electrodes and is the typical signature of the electrocatalytic H_2-oxidation activity of hydrogenases measured by protein film voltammetry. It is due to the inactivation of hydrogenases at high redox potentials and their subsequent reactivation when the potential is decreased.[47,48] The position of the inflection point of the reactivation process in the reverse scan has been defined as the switch potential (E_{switch}).[47] It has been shown that its value depends on the scan rate of the CV measurement and on thermodynamic (formal potential of the equilibrium between the active and inactive redox states of the hydrogenase bimetallic active site) and kinetic parameters (the rate constant of the inactive state reduction) of the reactivation process.[48] The E_{switch} value measured from the CV of the immobilized *D. vulgaris* Ni−Fe−Se hydrogenase in Figure 5b is approximately 0 mV, which is in the range of the values measured for other fast-reactivating hydrogenases.[8,48,49] Although a strict comparison of our result with the protein film voltammetry results reported for other hydrogenases is not possible because of the differences in the electrode geometry, immobilized enzyme architecture, and mass-transfer regimen of the CV measurement, we can conclude that the electrocatalytic currents measured in our modified gold electrodes correspond without doubt to the H_2-oxidation activity of the immobilized hydrogenase.[50]

Fluorescence Microscopy and FRAP Measurements. To obtain further proof of fluid-supported lipid bilayers being assembled on the gold surface and also on top of the hydrogenase molecules, samples containing 2% DiI fluorophore were observed with an epifluorescence microscope. Fluorescence microscopy images showed an almost homogeneous surface for both membranes (on top of 4-ATP modified gold and on top of immobilized hydrogenase molecules) with a few defects attributed to some liposomes adsorbed on the surface and/or small crystals of the fluorophore (data not shown). Figure 6a shows a fluorescence recovery of 90% 10 min after the end of photobleaching for the membrane on a 4-ATP gold surface. This confirms the

dx.doi.org/10.1021/la200141t |*Langmuir* 2011, 27, 6449–6457

fluidity of the membrane as well as the phospholipids' long-range motion. A mean value of the diffusion coefficient, D, for a phospholipid motion of $1.6 \pm 0.7\ \mu m^2\ s^{-1}$ was measured from three trials. In the case of the membrane formed on top of the hydrogenase monolayer, an almost complete recovery of fluorescence (~95%) was observed after 10 min (Figure 6b). The diffusion coefficient measured from three experiments was $3.6 \pm 0.5\ \mu m^2\ s^{-1}$. These two values of D are of the same order of magnitude as for other fluid lipid bilayers.[51,52] The higher value detected for the membrane on top of the hydrogenase monolayer could be due to the perturbation caused by the insertion of the protein lipid tails or the suppression of the electrode−phospholipid interaction. In any case, the diffusion coefficient measured is strong evidence that a fluid and a continuous lipid bilayer are formed on top of the hydrogenases anchored to the 4-ATP-modified gold.

CONCLUSIONS

A strategy for immobilizing a membrane hydrogenase onto gold surfaces with a controlled orientation in a fully active conformation has been developed. A two-step immobilization procedure leads to the insertion of the hydrogenase by its lipidic tail onto a phospholipidic bilayer formed over the gold surface. In such an orientation, the surface redox center of the protein is oriented toward the solution rather than toward the electrode. However, the one-step immobilization procedure favors the orientation of the hydrogenase molecules with the surface redox center facing the gold surface and the lipidic tail inserted into a phospholipid bilayer formed on top of the hydrogenase monolayer. The electrochemical measurements indicate that the first procedure allows only for mediated electron transfer from hydrogenase to the gold surface whereas the second method allows for direct electron transfer. The combined AFM and electrochemical study presented in this work is a useful tool for determining structure/function correlations of bioelectronic devices.

ASSOCIATED CONTENT

Supporting Information. AFM and electrochemical characterization of the covalent immobilization of the membrane hydrogenase to 4-ATP-modified gold without phospholipids, additional AFM images of hydrogenase and phospholipid coimmobilization on gold surfaces, and an electrochemical study of the permeability toward redox mediators of the phospholipid bilayer formed over the 4-ATP-modified gold surface. This material is available free of charge via the Internet at http://pubs.acs.org.

AUTHOR INFORMATION

Corresponding Author

*E-mail: alopez@icp.csic.es.

Author Contributions

[||]These authors contributed equally to this work.

ACKNOWLEDGMENT

This work was supported by the MICINN (projects CTQ2009-12649 and CONSOLIDER INGENIO 2010 CSD2007-00010, Spain), by a research grant (PTDC/BIA-MIC/104030/2008) funded by Fundação para a Ciência e Tecnologia (FCT, MCES, Portugal), and by a Luso-Spanish Joint Action funded by CRUP (Conselho de Reitores das Universidades Portuguesas, Portugal) and the MICINN (AIB2010PT-00367, Spain). D.O. acknowledges the JAE program from CSIC. We thank Dr. M. Pita for useful discussions.

REFERENCES

(1) Armstrong, F. A. *Curr. Opin. Chem. Biol.* **2005**, *9*, 110–117.
(2) Leger, C.; Bertrand, P. *Chem. Rev.* **2008**, *108*, 2379–2438.
(3) Willner, I; Katz, E. *Angew. Chem., Int. Ed.* **2000**, *39*, 1180–1218.
(4) Heller, A. *Phys. Chem. Chem. Phys.* **2004**, *6*, 209–216.
(5) Jeuken, L. J. C. *Nat. Prod. Rep.* **2009**, *26*, 1234–1240.
(6) Heffron, K.; Leger, C.; Rothery, R. A.; Weiner, J. H.; Armstrong, F. A. *Biochemistry* **2001**, *40*, 3117–3126.
(7) Zu, Y.; Shannon, R. J.; Hirst, J. *J. Am. Chem. Soc.* **2003**, *125*, 6020–6021.
(8) Goldet, G.; Wait, A. F.; Cracknell, J. A.; Vincent, K. A.; Ludwig, M.; Lenz, O.; Friedrich, B.; Armstrong, F. A. *J. Am. Chem. Soc.* **2008**, *130*, 11106–11113.
(9) Marchal, D.; Pantigny, M.; Laval, J. M.; Moiroux, J.; Bourdillon, C. *Biochemistry* **2001**, *40*, 1248–1256.
(10) Jeuken, L. J. C.; Connell, S. D.; Henderson, P. J. F.; Gennis, R. B.; Evans, S. D.; Bushby, R. J. *J. Am. Chem. Soc.* **2006**, *128*, 1711–1716.
(11) Infossi, P.; Lojou, E.; Chauvin, J. P.; Herbette, G.; Brugna, M.; Giudici-Orticoni, M. T. *Int. J. Hydrogen Energy* **2010**, *35*, 10778–10789.
(12) De Lacey, A. L.; Fernandez, V. M.; Rousset, M.; Cammack, R. *Chem. Rev.* **2007**, *107*, 4304–4330.
(13) Cracknell, J. A.; Vincent, K. A.; Armstrong, F. A. *Chem. Rev.* **2008**, *108*, 2439–2461.
(14) Yaropolov, A. I.; Karyakin, A. A.; Varfolomeev, S. D.; Berezin, I. V. *Bioelectrochem. Bioenerg.* **1984**, *12*, 267–274.
(15) Butt, J. N.; Filipiak, M.; Hagen, W. R. *Eur. J. Biochem.* **1997**, *245*, 116–122.
(16) Pershad, H. R.; Duff, J. L. C.; Heering, H. A.; Duin, E. C.; Albracht, S. P. J.; Armstrong, F. A. *Biochemistry* **1999**, *38*, 8992–8999.
(17) Hoeben, F. J. M.; Meijer, F. S.; Dekker, C.; Albracht, S. P. J.; Heering, H. A.; Lemay, S. G. *ACS Nano* **2008**, *2*, 2497–2504.
(18) Hoeben, F. J. M.; Heller, I.; Albracht, S. P. J.; Dekker, C.; Lemay, S. G.; Heering, H. A. *Langmuir* **2008**, *24*, 5925–5931.
(19) Mege, R. M.; Bourdillon, C. *J. Biol. Chem.* **1985**, *260*, 4701–4706.
(20) Rüdiger, O.; Abad, J. M.; Hatchikian, E. C.; Fernandez, V. M.; De Lacey, A. L. *J. Am. Chem. Soc.* **2005**, *127*, 16008–16009.
(21) Eng, L. H.; Elmgren, M.; Komlos, P.; Nordling, M.; Lindquist, S. E.; Neujahr, H. Y. *J. Phys. Chem.* **1994**, *98*, 7068–7072.
(22) Morozov, S. V.; Karyakina, E. E.; Zorin, N. A.; Varfolomeyev, S. D.; Cosnier, S.; Karyakin, A. A. *Bioelectrochemistry* **2002**, *55*, 169–171.
(23) De Lacey, A. L.; Detcheverry, M.; Moiroux, J.; Bourdillon, C. *Biotechnol. Bioeng.* **2000**, *68*, 1–10.
(24) Lojou, E.; Bianco, P. *Electroanalysis* **2006**, *18*, 2426–2434.
(25) Alonso-Lomillo, M. A.; Rüdiger, O.; Maroto-Valiente, A.; Velez, M.; Rodriguez-Ramos, I.; Muñoz, F. J.; Fernandez, V. M.; De Lacey, A. L. *Nano Lett.* **2007**, *7*, 1603–1608.
(26) Rüdiger, O.; Gutiérrez-Sánchez, C.; Olea, D.; Pereira, I. A. C.; Vélez, M.; Fernández, V. M.; De Lacey, A. L. *Electroanalysis* **2010**, *22*, 776–783.
(27) Volbeda, A.; Charon, M. H.; Piras, C.; Hatchikian, E. C.; Frey, M.; Fontecilla-Camps, J. C. *Nature* **1995**, *373*, 580–587.
(28) Valente, F. M. A.; Oliveira, A. S. F.; Gnadt, N.; Pacheco, I.; Coelho, A. V.; Xavier, A. V.; Teixeira, M.; Soares, C. M.; Pereira, I. A. C. *J. Biol. Inorg. Chem.* **2005**, *10*, 667–682.
(29) Gutiérrez-Sánchez, C.; Rüdiger, O.; Fernández, V. M.; De Lacey, A. L.; Marques, M.; Pereira, I. A. C. *J. Biol. Inorg. Chem.* **2010**, *15*, 1285–1292.
(30) Valente, F. M. A.; Pereira, P. M.; Venceslau, S. S.; Regalla, M.; Coelho, A. V.; Pereira, I. A. C. *FEBS Lett.* **2007**, *581*, 3341–3344.
(31) Marques, M.; Coelho, R.; Pereira, I. A. C.; Matias, P. M. *Acta Crystallogr., Sect. F: Struct. Biol. Crust. Commun.* **2009**, *65*, 920–922.

(32) Macdonald, R. C.; Macdonald, R. I.; Menco, B. P. M.; Takeshita, K.; Subbarao, N. K.; Hu, L. R. *Biochim. Biophys. Acta* **1991**, *1061*, 297–303.
(33) D.M. Soumpasis, D. M. *Biophys. J.* **1983**, *41*, 95–97.
(34) Wang, X.; Shindel, M. M.; Wang, S. W.; Ragan, R. *Langmuir* **2010**, *26*, 18239–18245.
(35) Cha, T.; Athena, G.; Zhu, X. Y. *Biophys. J.* **2006**, *90*, 1270–1274.
(36) Bryant, M. A.; Crooks, R. M. *Langmuir* **1993**, *9*, 385–387.
(37) Garcia-Manyes, S.; Gorostiza, P.; Sanz, F. *Anal. Chem.* **2006**, *78*, 61–70.
(38) Quist, A. P.; Chand, A.; Ramachandran, S.; Daraio, C.; Jin, S.; Lal, R. *Langmuir* **2007**, *23*, 1375–1380.
(39) Garcia-Manyes, S.; Sanz, F. *Biochim. Biophys. Acta* **2010**, *1798*, 741–749.
(40) Allen, T. M.; Romans, A. Y.; Kercret, H.; Segrest, J. P. *Biochim. Biophys. Acta* **1980**, *601*, 328–342.
(41) Marques, M. C.; Coelho, R.; De Lacey, A. L.; Pereira, I. A. C.; Matias, P. M. *J. Mol. Biol.* **2010**, *396*, 893–907.
(42) Nakamura, C.; Mizutani, W.; Lantz, M. A.; Noda, K.; Zorin, N. A.; Miyake, J. *Supramol. Sci.* **1998**, *5*, 639–642.
(43) Levy, D.; Chami, M.; Rigaud, J. L. *FEBS Lett.* **2001**, *504*, 187–193.
(44) de la Maza, A.; Parra, J. L. *Colloid Polym. Sci.* **1996**, *274*, 253–260.
(45) Green, J. D.; Kreplak, L.; Goldsbury, C.; Blatter, X. L.; Stoltz, M.; Cooper, G. S.; Seelig, A.; Kistler, J.; Aebi, U. *J. Mol. Biol.* **2004**, *342*, 877–887.
(46) Teixeira, M.; Moura, I.; Fauque, G.; Dervartanian, D. V.; LeGall, J.; Peck, H. D.; Moura, J. J. G.; Huynh, B. H. *Eur. J. Biochem.* **1990**, *189*, 381–386.
(47) Jones, A. K.; Lamle, S. E.; Pershad, H. R.; Vincent, K. A.; Albracht, S. P. J.; Armstrong, F. A. *J. Am. Chem. Soc.* **2003**, *125*, 8505–8514.
(48) Fourmond, V.; Infossi, P.; Giudici-Orticoni, M. T.; Bertrand, P.; Leger, C. *J. Am. Chem. Soc.* **2010**, *132*, 4848–4857.
(49) Parkin, A.; Goldet, G.; Cavazza, C.; Fontecilla-Camps, J. C.; Armstrong, F. A. *J. Am. Chem. Soc.* **2008**, *130*, 13410–13416.
(50) The fact that inactivation of the hydrogenase is observed in the CV with the gold wire and not in CV of the gold plate indicates that in the first case the enzymatic reaction rate limits the electrocatalytic process whereas it does not in the second case. However, we do not have a clear explanation of this difference in electrocatalytic behavior between the two types of electrodes.
(51) Adalsteinsson, T.; Yu, H. *Langmuir* **2000**, *16*, 9410–9413.
(52) Weng, K. C.; Kanter, J. L.; Robinson, W. H.; Frank, C. W. *Colloids Surf., B* **2006**, *50*, 76–84.